Journal of Multidisciplinary Engineering Science Studies (JMESS)
ISSN: 2458-925X
Vol. 2 Issue 9, September - 2016

Nanoparticle dopants TiO_2 films for structure, optical and gas sensing properties prepared by PLD technique

Ali Ahmed Yousif
Department of Physics, College of Education, University of Al-Mustansiriyah, Baghdad, Iraq
Corresponding author: ahmed_naji_abd@yahoo.com

***Abstract*—Nanoparticle TiO_2 doped with metals such as (Mn, NI, W and CO) thin films were prepared by Pulsed Laser Deposition (PLD) technique using pulsed Nd-YAG laser with wavelength (λ= 532 nm) and duration (7ns) and energy fluence (1.6 J/cm^2) on glass substrates. The structural and optical properties of these films have been investigated using XRD, AFM, and UV-Visible spectroscopy in the wavelength range (320–1100) nm. The XRD results showed that all films are polycrystalline in nature with tetragonal structure and preferred orientation along (110), (101), (210), (310) and (202) peaks at Rutile phase of respectively, and peaks (112) plane at Anataes phase. The crystallite size was calculated using Scherrer formula. XRD pattern shows an decrease in the average size of the crystalline grains with the range (5.75-23.8)nm in the all film samples. The morphology and topography of the surface were determined Scanning Electron Microscope (SEM) and Atomic Force Microscopy (AFM) technique, which shows that the grain size of the nanoparticle observed at the surface depend on the type of metals dopant. TiO_2 doped with 5% Co metal has the smallest grain size of (32.68nm) and RMS values (4.22nm). The optical properties of the films are studied the transmittance measurements have shown that our films are highly transparent in the visible and infrared wavelength region, an average transmittance of ~ 90% for undoped TiO_2 thin films decreases with the increasing of dopants. The optical band gap of the films is found to be 3.72eV for pure TiO_2, and decreases at doping from 3.60 eV to 3.35 eV.**

The produced thin films in this have been exposed to 80ppm NO_2 gas concentration, TiO_2 deped with metal has sensitivity of higher than pure TiO_2 .TiO_2 deped with W metal deposited on glass has 80.2% maximum sensitivity to NO_2 gas with optimum temperature of 250°C.

Keywords—Pulsed laser deposition, Nanoparticle TiO_2, Structural, Optical and sensitivity properties.

1. Introduction

Titanium dioxide has gain interest as apromising semiconductor material due to its peculiar properties such as non-toxicity, high catalytic efficiency [1]. TiO_2 has been employed in many fields such as photo-catalysis, gas sensing, organic dye-sensitized solar cells, water-splitting [2-4]. It has been found in three crystallographic phases , anatase, rutile, and brookite [5]. The photocatalytic properties of TiO_2 were limited because of its large band gap (3.3 eV). TiO_2 doping with some nonmetal elements such as nitrogen is a suitable method, which would enhance the optical response of TiO_2 to the visible area [6]. Newly, oxide supported Au nanoparticles have involved significant attention due to the catalytic activities of these materials at low temperatures [7,8].

Doping of TiO_2 has been an important approach in band gap engineering to change the optical response of semiconductor photocatalysts. The main objective of doping is to induce a bath chromic shift, *i.e*., a decrease of the band gap or introduction of intra-band gap states, which results in the absorption of more visible light. Doping may lead to photocatalytic systems that exhibit enhanced efficiency [9]. It is desirable to maintain the integrity of the crystal structure of the photocatalyst while changing its electronic structure by doping. It is easier to replace Ti^{4+} in TiO_2 with a cation than to substitute O^{2-} with another anion because of the difference in the charge states and ionic radii [10]. Nanomaterials show a higher tolerance to structural distortion than bulk materials due to their inherent lattice strain. As a result, the surface modification of TiO_2 nanoparticles appears to be more beneficial than the modification of bulk TiO_2 [11]. The object of this work, we report the successful growth of doped and undoped TiO_2 nanoparticles on glass substrates by pulsed laser deposition technique. Besides the structure, morphology, topography and optical properties as a function of dopant metals, we investigated the gas sensor properties of the deposited thin films.

2. Experiment work

The deposition was carried out using Q-switched Nd-YAG laser with a frequency second radiation at λ= 532 nm (pulse width 7ns repetition rate 10 HZ) and fluencies energy (1.6 J/cm^2). The studied films were prepared by from nanoparticle TiO_2-pur and (5 wt%) (Mn, NI, W and CO) doped TiO_2 targets films were grown by (PLD) technique deposition on optically flat on glass substrates kept an on-axis distance of 4cm from the TiO_2 target. The chamber was kept at vacuum pressure of 10^{-3} mbar as shown in figure (1). The TiO_2 disc was ablated from 200 pulses (15min) to get single layered thin films.

During the deposition the substrate temperatures were kept at 400^{o}C under 5x10^{-1}mbar oxygen pressure.

.

1. Nd: YAG Laser Head.
2. Quartz Chamber.
3. Stainless steel Flange.
4. Vacuum system
5. Flexible tube KF16
6. Substrate holder
7. Variac devices
8. Power supply Nd:YAG laser

Figure (1): Pulsed laser deposition (PLD) system

3. Characterization of thin films

The polycrystalline structure of the films was analyzed with X-Ray Diffraction (XRD, Rigakn DMAX 2800), power diffraction system with Cu-Kα x-ray tube (λ=1.54056 Å) was used. The X-ray scans were performed between 2θ values of 10° and 120°.

The microstructures of the films were analyzed using Scanning Electron Microscope, (SEM, JEOL JED 2300) and by Atomic Force Microscopy (AFM-Digital Instruments Nan Scope) working in tapping mode. Thickness measurements were carried out using a He-Ne laser at λ=362nm, the thicknesses of the films were observed in the of (200nm). The absorption spectra of undoped and with metals (Mn, NI, W and CO) thin films were studied by UV-visible (Perkin Elemer Company) spectrophotometer in spectral range of (320-1100)nm. The data from transmission spectrum could use in the calculation of the absorption coefficient (α) by using the following equation [12]:

$$\alpha = \frac{1}{d} \ln \frac{1}{T} \quad \ldots\ldots. (1)$$

Where d: is the thickness of thin film, and T is the transmission.The absorption coefficient (α) and optical energy gap (Eg) are related by [13]:

$$\alpha h\nu = A(h\nu - Eg)^n \quad \ldots..(2)$$

Where A: is constant depending on transmission probability, h: is Plank's constant , ν: is the frequency of the incident photon, Eg: is the energy gap of the material and n has different values depending on the nature of absorption process. The sensing measurements were carried out by measuring the variation in (resistivity and

conductivity) through measuring the output current resulting from exposing the thin film surface to the gas or chemical vapor (NO_2) Nitrogen dioxide (laboratory reagents 99.9%), were evaporated by heating them to (50^{o}C), the temperature was recorded by a k-type thermocouple (XB 9208B). The bias voltage was supplied by (FARNELL E350) power supply. The output current was recorded by (Kithley-619 Electrometer) multimeter. The thin film surface exposed to 80 ppm vapor concentrations of NO_2. The measuring carried out with an applied voltage constant to 6 volts at temperatures range of (50-450^{o}C).

4. Results and Discussion

Nanoparticle TiO_2 doped with metals (Mn, NI, W and CO) at percent (5wt.%) under $5x10^{-1}$mbar oxygen pressure, 400^{o}C substrate temperatures and 1.6 J/cm^2 laser fluence on glass substrates are shown in figure (2). At TiO_2-pure, the film shown diffraction peaks located at 2θ=27.50°, 36.25°, 44.30°, 64.67° and 77.69°, which belong to Rutile (110), (101), (210), (310) and (202) peaks respectively, according to standard pattern of Rutile TiO_2, and appearance of Anataes peaks (112) at 2θ=38.14°, can be observed in the x-ray profile of pure TiO_2 film as shown in table (1). The existence of Rutile phase in TiO_2 could lowering the photo-catalytic activity of both the doped catalysts and increase reflectivity. From figure shown the doped TiO_2 films diffraction at 5wt.% concentration of metals the all peaks of Rutile decreasing and (FWHM) increasing, while observed of Anataes peaks A(112) and (FWHM) increasing for all metals doped TiO_2 films as shown in figure (2).The full width at half maximum (FWHM) of the Rutile and Anataes peaks were also evaluated to analyze the variation of grain sizes in the films doped, were observed from TiO_2- pure and TiO_2 doped with metals (Mn, NI, W and CO) films generally have smaller grain sizes, as shown in table (1). The doping metals of might have to the increased potential energy of atomic diffusion barrier and further results in the inhibition of Rutile and Anataes transition and grain growth. Overall, it can be note that all XRD patterns of nanoparticle TiO_2 and doped TiO_2 films did not show any Important changes. These results indicated that dopants have no effect on the Rutile and Anataes structure of TiO_2 films. XRD analysis also did detect the dopant phase. Where, no dopant peak can be observed in this research when the dopants concentration was (5wt.%).

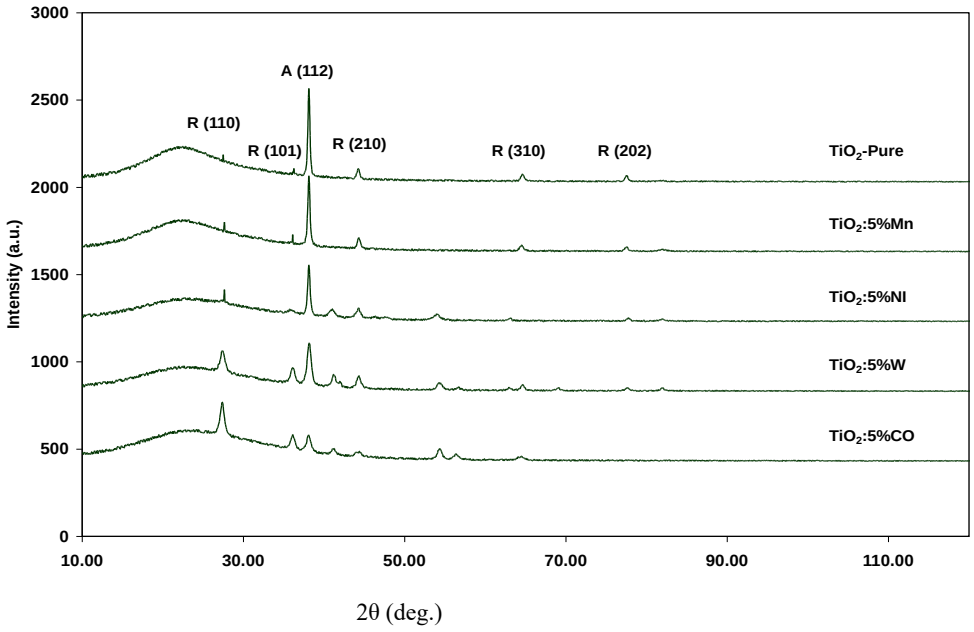

Figure 2. X-ray diffraction (XRD) pattern measured for Nanoparticle TiO_2-pure and doped with metals (Mn, NI, W and CO) at percent (5wt.%), (A: anatase phase, R: rutile phase).

Table (1) The obtained result of the structural parameters from XRD for Nanoparticle TiO_2-pure and doped with metals (Mn, NI, W and CO) at percent (5wt.%)

Samples	2θ (Deg.)	d_{hkl} Std.(Å)	d_{hkl} Exp.(Å)	G.S (nm)	FWHM (Deg.)	Phase	hkl	Card No.
TiO_2-Pure	27.50	3.24	3.24	22.45	0.43	Rutile	(110)	21-1276
	36.25	2.48	2.49	20.44	0.46	Rutile	(101)	21-1276
	38.14	2.33	2.32	12.23	0.61	Anataes	(112)	21-1272
	44.30	2.05	2.10	23.80	0.42	Rutile	(210)	21-1276
	64.67	1.45	1.46	18.11	0.48	Rutile	(310)	21-1276
	77.69	1.24	1.25	16.76	0.50	Rutile	(202)	21-1276
TiO_2:5%Mn	27.64	3.24	3.25	18.21	0.48	Rutile	(110)	21-1276
	36.11	2.48	2.47	16.67	0.51	Rutile	(101)	21-1276
	38.56	2.33	2.32	9.21	0.64	Anataes	(112)	21-1272
	44.44	2.05	2.06	21.84	0.45	Rutile	(210)	21-1276
	64.67	1.45	1.46	15.14	0.52	Rutile	(310)	21-1276
	77.76	1.24	1.23	15.88	0.50	Rutile	(202)	21-1276
TiO_2:5%NI	27.68	3.24	3.26	12.88	0.61	Rutile	(110)	21-1276
	36.18	2.48	2.47	14.56	0.53	Rutile	(101)	21-1276
	38.14	2.33	2.32	8.21	0.65	Anataes	(112)	21-1272
	44.37	2.05	2.09	18.82	0.48	Rutile	(210)	21-1276
	64.05	1.45	1.47	15.14	0.49	Rutile	(310)	21-1276
	77.99	1.24	1.23	13.26	0.54	Rutile	(202)	21-1276
TiO_2:5%W	27.50	3.24	3.22	11.43	0.62	Rutile	(110)	21-1276
	36.32	2.48	2.48	14.06	0.54	Rutile	(101)	21-1276
	38.21	2.33	2.36	7.98	0.67	Anataes	(112)	21-1272
	44.44	2.05	2.04	17.55	0.49	Rutile	(210)	21-1276
	64.95	1.45	1.44	14.12	0.53	Rutile	(310)	21-1276
	77.62	1.24	1.25	12.28	0.62	Rutile	(202)	21-1276
TiO_2:5%CO	27.50	3.24	3.26	8.55	0.68	Rutile	(110)	21-1276
	36.11	2.48	2.47	11.33	0.63	Rutile	(101)	21-1276
	38.21	2.33	2.31	5.75	0.69	Anataes	(112)	21-1272
	44.58	2.05	2.12	14.15	0.54	Rutile	(210)	21-1276
	64.60	1.45	1.46	12.19	0.62	Rutile	(310)	21-1276
	77.91	1.24	1.23	10.44	0.63	Rutile	(202)	21-1276

Characterization and testing-Scanning electron microscopy (SEM) were used to study the change in the structural morphology of the anodized thin film with change in doped. All the top view micrographs were obtained at 10.00kx magnification, The SEM micrographs of the nanoparticle TiO_2 doped with metals (Mn, NI, W and CO) films at percent (5wt.%). Figure (3), it can be seen that the morphology of the undoped TiO_2 film is completely different from those of doped TiO_2 films. In general, all the doped TiO_2 films consist of nanosized primary particles with spherical shape in agglomerated nanoparticles, whereas, the pure TiO_2 film consists of relatively larger (Compared with the doped) chunks of nanoparticles. The pure undoped TiO_2 film consists of about ~90 nm size. A close look into these thin films micrographs reveals that the degree of agglomeration increased with the doping of metals (Mn, NI, W and CO) films. The particles of the doped TiO_2 films are finer of about (~50 nm) at percent (5wt.%).

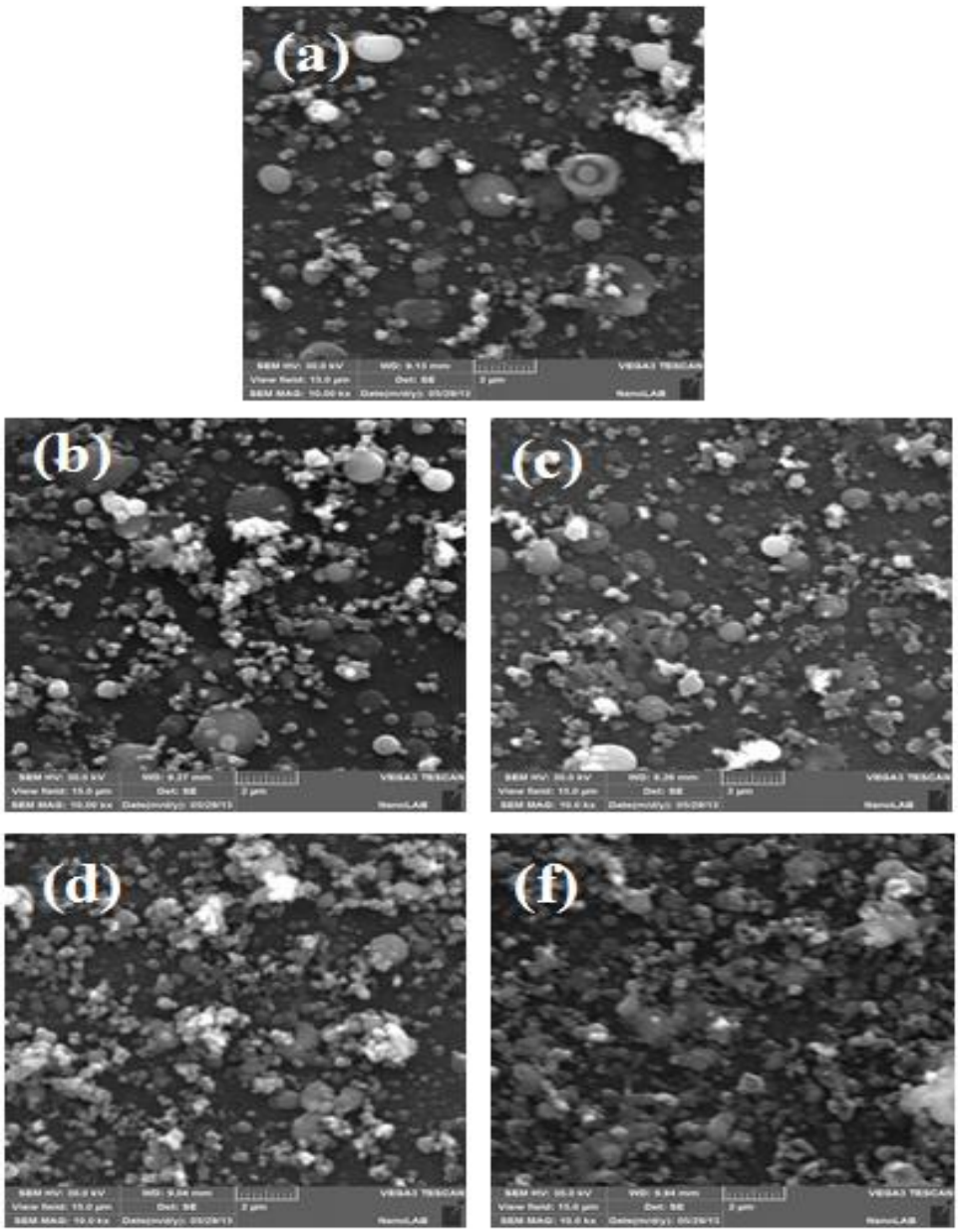

Figure 3. SEM micrographs showing the change is the morphology of Nanoparticle TiO_2-pure with the change of doping at (a) pure, (b) 5%Mn, (c) 5%NI, (d) 5%W and (e) 5%CO

The AFM image of TiO_2 nanoparticle doped with metals sample are shown in figure (4).under a fixed substrate temperatures of 400^oC , oxygen pressure of ($5x10^{-1}$mbar) and (1.6 J/cm^2) fluencies energy density. AFM image of Mn, NI, W and CO doped TiO_2 thin films show a uniform spherical shape The size diameter was evaluated from the plane view images at range (32.68-65.26nm). The tilted image reveals grain heights of a few tens of nanometers. Surface roughness increases with metal percent due the presence of the fine dispersed phase. The samples are very rough with Root Mean Square (RMS) values (2.24, 3.39, 4.46, 5.19and 4.22) for undoped thin films and doping with 5% (Mn, NI, W and CO) respectively as shown in table (2).

***Table (2) The obtained result of the topography surface from AFM image for Nanoparticle TiO_2-pure and doped with metals (Mn, NI, W and CO) at percent* (5wt.%)**

Samples	RMS (nm)	RS (nm)	Ten point height (nm)	g.s (nm)
TiO_2 - Pure	2.24	1.21	1.88	65.26
TiO_2:5%Mn	3.39	2.07	4.15	44.97
TiO_2:5% NI	4.46	5.85	12.4	48.23
TiO_2:5% W	5.19	7.01	13.22	42.55
TiO_2:5% CO	4.22	5.64	12.12	32.68

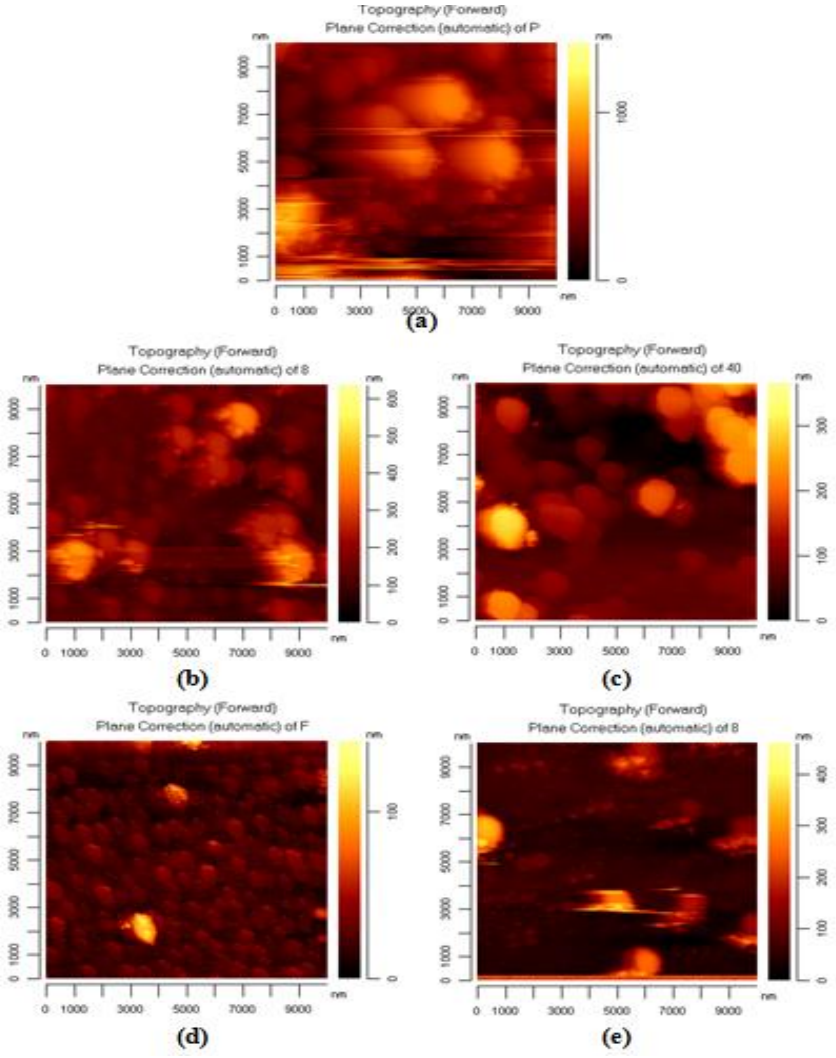

Figure 4. AFM image showing the change is the topography of Nanoparticle TiO_2-pure with the change of doping at (a) pure, (b) 5%Mn, (c) 5%NI, (d) 5%W and (e) 5%CO

Figure (5), shows the relation between transmittance and wavelength in the range of (320 - 1100 nm) for nanoparticle TiO_2 doped with metals (Mn, NI, W and CO) films at percent (5wt.%). The transmittance for all thin films increases rapidly as the wavelength increases in the range of (320- 360 nm), and then increases slowly at higher wavelengths. The spectrum shows high transmittance in the visible and infrared regions, and low in the ultraviolet region. Also, ones can observe in this figure that the fundamental absorption edge (absorption edge which separates the high absorption region and the low absorption region or the window region) is sharp in the ultraviolet region at the wavelength (370 nm) of the spectrum. The maximum transmittance observed of undoped TiO_2 thin films was about 90%, Also note of Figure (5) show the transmittance decreases with increase in the doping. The doped Mn has a maximum transmittance of nearly equal to 78%, and a minimum transmittance of about 71% for CO thin films.

For all the films, high transmission shown at long wavelengths, the doped sample records the high transmittance across the considered spectrum. The effect of doping on the transmission of TiO_2 films can be linked with decreasing in partical size.

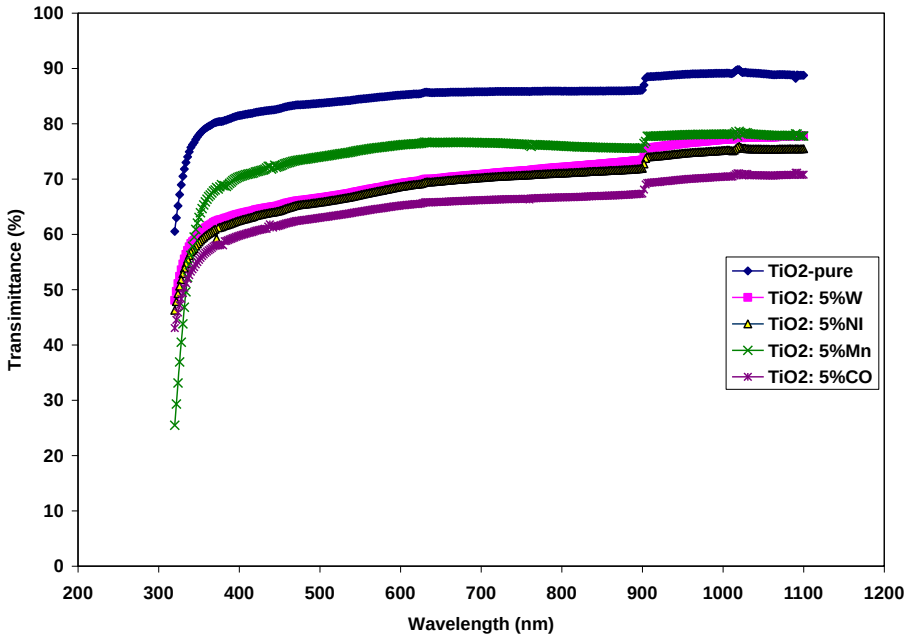

Figure (5): Transmittance (%) versus wavelength (λ) of Nanoparticle TiO_2-pure thin films at different dopants.

The energy gap values depend in general on the films crystal structure, the arrangement and distribution of atoms in the crystal lattice, also affected by crystal regularity. The optical energy gap (Eg) was derived assuming allowed direct transitions between the edge of the valence and conduction band. The energy gap was calculated using equation (2) where r=1/2 for allowed direct

transitions for nanoparticle TiO_2 doped with metals (Mn, NI, W and CO) films, by plotting a graph between $(\alpha h\nu)^2$ and ($h\nu$) in eV, a straight line is obtained which gives the value of the direct band gap. The extrapolation of the straight line to $(\alpha h\nu)^2=0$ gives value of the direct band gap of the material, and this could be seen in figure (6). Ones notice that the band gap value decreases when the doping metals increases, the allowed direct band gap values range between 3.72eV to 3.35 eV for the prepared samples, as shown in table (3).

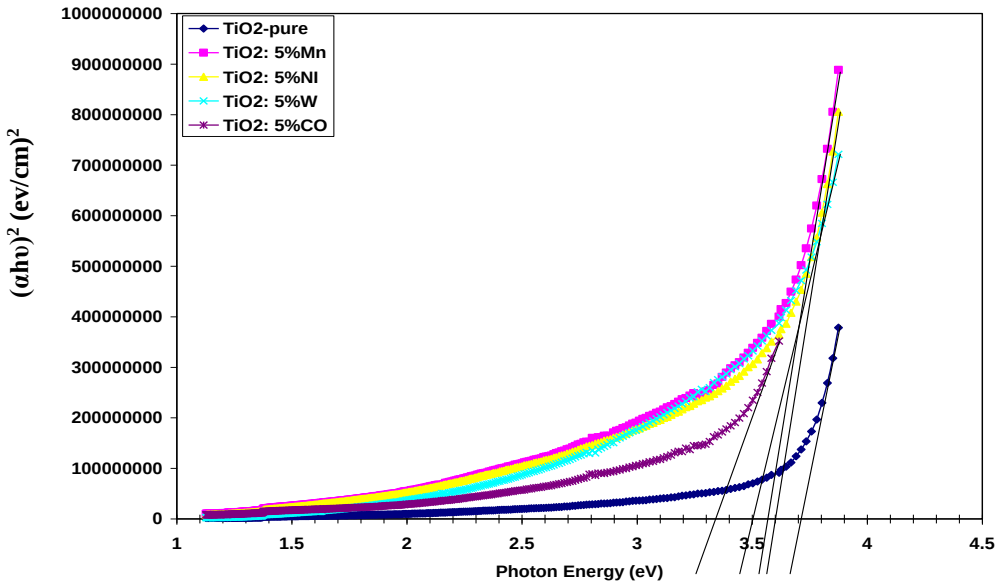

Figure (6): The relation between $(\alpha h\upsilon)^2$ and $(h\upsilon)$ of Nanoparticle TiO_2-pure thin films at different dopants.

Table 3. Bandgap values for Nanoparticle TiO_2-pure thin films at different dopants.

Samples	Eg (eV)
TiO_2 - Pure	3.72
TiO_2:5%Mn	3.6
TiO_2:5% NI	3.57
TiO_2:5% W	3.5
TiO_2:5% CO	3.35

Figure (7) shows the sensitivity as a function of operation temperature in the range (50-450^oC) for nanoparticle TiO_2 doped with metals (Mn, NI, W and CO) films at concentration (5wt.%), which are deposited on glass substrate at oxygen pressure of ($5x10^{-1}$mbar) and (1.6 J/cm^2) fluencies energy density. The sensing test was done using 3% NO_2: air mixed ratio and bias voltage (6V) were applied on the electrodes of all samples at 80 ppm of NO_2.

It can be seen from figure that the sensitivity of all the films increases with the increasing in the operation temperature, reaching a maximum value corresponding to an optimum operation temperature which in 250^{o}C for all the samples. Above this temperature the sensitivity to NO_2 gas for all samples decreases. The high operation temperature of the sensor make the life time of the sensor become shorter and increasing resistance thus required more electricity for operation. It is believed that the oxygen could be removed or lost from the bulk of the metal oxide materials at high temperature. This suggests that the response of the sensor may decrease at higher temperature since there will be more oxygen vacancies which led to less occurrence of NO_2 oxygen reaction. The response of the undoped sensor to NO_2 gas is relatively low, and the maximum response is (41%) at 250^{o}C. Metals doping (Mn, NI, W and CO) increases the sensitivity of TiO_2 sensor to NO_2 gas and improves the sensor response at which the sensor response is maximized (80.2%) at 250^{o}C for TiO_2 doping tungsten (W). the sensing process depends on the surface roughness which increases detection sensitivity doping TiO_2 films have higher value of sensitivity from pure TiO_2 because the surface roughness of doping TiO_2 higher than pure TiO_2. table (4) shows the sensitivity surface roughness values of TiO_2-pure and doping with metals (Mn, NI, W and CO) films at concentration (5wt.%) at operation temperature 250^{o}C.

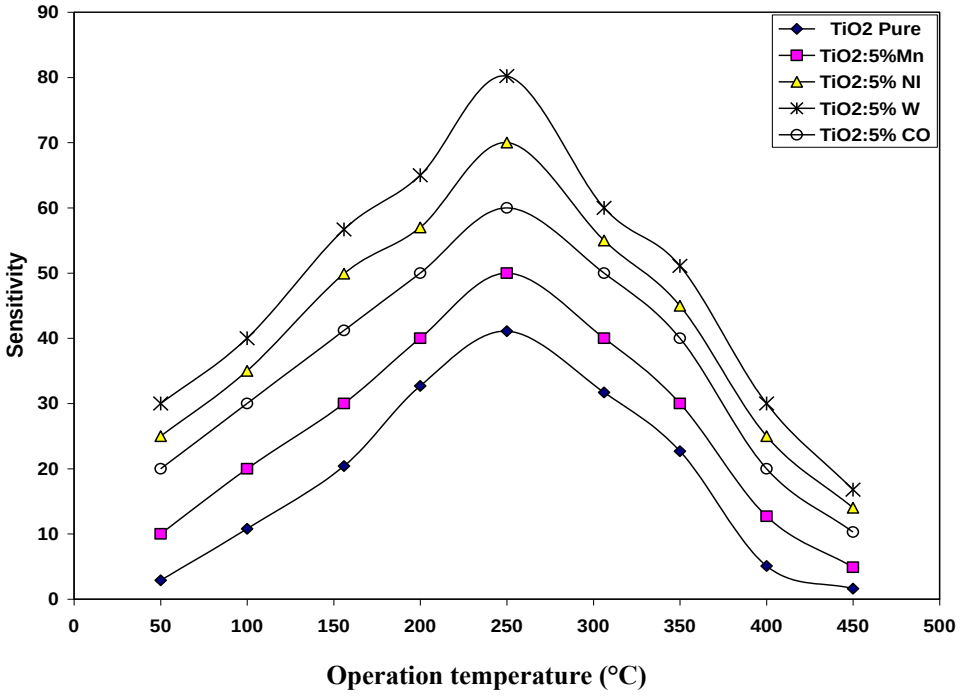

Figure (7): Sensitivity for TiO_2 pure and doping with 5% (Mn, NI, W and CO) films for NO_2 gas at different operation temperature.

Table 4. Sensitivity values of TiO_2 pure and doping with different metals at operation temperature (250ºC).

Samples	Sensitivity %	RS (nm)
TiO_2 - Pure	41.1	1.21
TiO_2:5%Mn	49.5	2.07
TiO_2:5% NI	70.0	5.85
TiO_2:5% W	80.2	7.01
TiO_2:5% CO	61.2	5.64

5.Conclusions

In this work, we have successfully prepared undoped and doped metals (Mn, NI, W and CO) films with concentration of (5wt.%) on glass substrates by Pulse laser deposition method.The XRD results showed that all films are polycrystalline in nature with a tetragonal structure and the with presence of Rutile - Anatase phase correlation for all films.The SEM and AFM studiy results showed a uniform spherical shape in nanoparticles surface morphology for TiO_2- pure and TiO_2 doped with metals (Mn, NI, W and CO) films, The results of grain size obtained from SEM and AFM investigation are qualitatively in agreement with those obtained from XRD analysis.The transmittance for all thin films increases rapidly as the wavelength increases in the range of (320-360 nm), and then increases slowly at higher wavelengths. so optical absorptance is high at short wavelength, therefore, the film is good to be detector within ultra-violet region range. The average transmittance of deposited undoped is about 90% in the visible and near-infrared region , and the transmittance decreases with increase in the doping. The optical bandgap of the undoped and TiO_2 doped with metals (Mn, NI, W and CO) films with Anatase - Rutile phase was lowered of 3.72 to 3.35 eV, respectively.From the obtained results, conclusions can be made for sensing performance of TiO_2 pure and dopant it with metals modified sensor. pure TiO_2 showed poor response to NO_2 gas. nanoparticle TiO_2 doped with metals (Mn, NI, W and CO) films at concentration (5wt.%) was the most sensitive element to NO_2 gas. The optimum operation temperature for NO_2 gas sensing was 250ºC. TiO_2 thin films doped with metals would be suitable for fabricating the NO_2 gas sensor. The sensor TiO_2 doping with tungsten (W) showed good Sensitivity to NO_2 gas.

References

1. R. Erdogan., O. Ozbek and I. Onal, 2010. A periodic DFT study of water and ammonia adsorption on anatase TiO_2 (001) slab. Journal of Surface science, 604:1029-1033.
2. M. Mirzaei, H. Ahadi, M. Shariaty-Niassar and M. Akbari, 2015. Fabrication and characterization of Visible Light active Fe-

doped Nanocomposites as Nanocatalyst. Int. J. Nanosci. Nanotechnol, 11(4): 289-293.

3. H. Zarei, M. Zeinali, H. Ghourchian and Kh. Eskandari, 2013. Gold Nano-particles as electrochemical signal amplifier for immune-reaction monitoring. Int. J. Nano. Dimens, 4(1): 69- 76.
4. M. Batzilla., E. H. Morales and U. Diebold, 2007. Surface studies of nitrogen implanted TiO_2, Journal of Chemical Physics, 339:36–43.
5. M. Bellardita., M. Addamo., A. Di Paola and L. Palmisano, 2007. Photocatalytic behaviour of metal loaded TiO_2 aqueous dispersions and films, Chemical Physics. 339:94– 103.
6. O. Zuas, H. Budiman and N. Hamim, 2013. Anatase TiO2 and mixed M-Anatase TiO_2 (M=CeO_2 or ZrO_2) nano powder: Synthesis and characterization. Int. J. Nano. Dimens, 4(1), 7-12.
7. M. K. Otoufi, N. shahtahmasebebi, A. Kompany and E. Goharshadi, 2014. A systematic growth of gold nanoseeds on Silica for Silica Gold core-shell nanoparticles and investigation of optical properties. Int. J. Nano. Dimens, 5(6): 525-531.

8. Amirali Abbasi, Jaber Jahanbin Sardroodi, Alireza Rastkar Ebrahimzadeh, 2016. TiO_2/Gold nanocomposite as an extremely sensitive molecule sensor for NO_2 detection: A DFT study, J. Water Environ. Nanotechnol., 1(1): 55-62.

9. Carp O, Huisman C L, Reller A. 2004, Photoinduced reactivity of titanium dioxide. Prog in Solid State Chem, 32: 33–117

10. Mor G K, Varghese O K, Paulose M, 2006, A review on highly ordered, vertically oriented TiO_2 nanotube arrays: Fabrication, material properties, and solar energy applications. Solar Energ Mater Solar Cell, 90: 2011–2075

11 Burda C, Lou Y, Chen X, 2003, Enhanced nitrogen doping in TiO_2 nanoparticles. Nano Lett, 3: 1049–1051

12. S. Dimitrijev, “Understanding Semiconductor Devices”, 2000, Copyright by Oxford University Press.

13. N.Al-Hardan , M.J.Abdullnh, 2009, Appl. Surf .Sci. 235, 7794-7797.